

COMPLETE ENERGY PROFILE OF A CHIRAL PROPELLER COMPOUND: TRIS-(2'-METHYLBENZIMIDAZOL-1'-YL)METHANE (TMBM). CHROMATOGRAPHIC RESOLUTION ON TRIACETYL CELLULOSE, X-RAY STRUCTURES OF THE RACEMIC AND ONE ENANTIOMER, AND DYNAMIC NMR STUDY

Concepción Foces-Foces, Félix Hernández Cano* and Martín Martínez-Ripoll
U.E.I. de Cristalografía, Instituto "Rocasolano", CSIC, Serrano 119,
28006 Madrid, Spain

Robert Faure and Christian Roussel

Département de Chimie & ESIPSOI, Université d'Aix-Marseille III, Centre
de Saint-Jérôme, 13397 Marseille Cédex 13, France

Rosa M^a Claramunt, Concepción López and Dionisia Sanz

Departamento de Química Orgánica, Facultad de Ciencias, UNED, Ciudad
Universitaria, 28040 Madrid, Spain

and José Elguero

Instituto de Química Médica, CSIC, Juan de la Cierva 3, 28006 Madrid, Spain

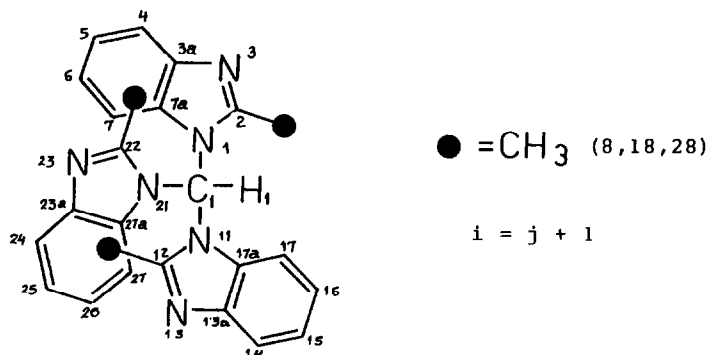
(Received 4 December 1989)

Tris-(2'-methylbenzimidazol-1'-yl)methane (TMBM) presents an interesting example of propeller-like chirality, which is discussed according to Mislow's and Dunitz's descriptions. Fortunately, the two most stable isomers (the three methyl groups "up", *i.e.* on the same side of the methine proton, and two methyl groups "up" and the third one "down") were present in the solid state, thus allowing the determination of their molecular structure by X-ray crystallography. The activation barrier which separates both isomers (9.8 kcal.mol⁻¹) was determined by dynamic ¹H n.m.r., whereas that corresponding to enantiomers (28.5 kcal.mol⁻¹) was determined kinetically by racemization, after pure enantiomers were resolved by chromatography on microcrystalline triacetyl cellulose. Both the racemic TMBM and its enantiomers crystallize with a larger number of water molecules, six and seven respectively, forming cyclic structures.

INTRODUCTION

Isomeric Forms and Nomenclature.- Tris-(2'-methylbenzimidazol-1'-yl)methane (TMBM) is a chemical system able to show stereoisomerism and, in particular, enantiomerism, due to restricted internal rotations. Moreover, it is a molecule which is able to adopt the so called "propeller" conformations: it has three fused ring systems, which can act as blades, attached to a methine group, thus producing a frame with D₃ symmetry.

This kind of system has been studied by Mislow *et al.*¹⁻³ Following their description, isomerism in this molecule arises from the sterically hindered rotation of the fused rings about the C(1)-N(j1) frame bond, and is measured by the torsion angles $\phi_1 \equiv \text{H}(1)-\text{C}(1)-\text{N}(j1)-\text{C}(j2)$. Regarding the chi-



rality elements used by Mislow *et al.*, in the case of TMBM there is no "chirality center" since the three substituents are equal.

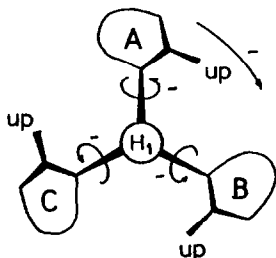
The relative position of the fused rings with regard to the plane of chirality, taking as + the side where H(1) is located, may be described, in terms of the torsion angles, as +, x \rightarrow (ϕ , ϕ , ϕ), +, a \rightarrow ($\phi \pm \pi$, ϕ , ϕ), and so on, ϕ having any value. Finally, the helical chirality, measured with regard to the C(1)-H(1) axis as zero position, is described by the sign of the ϕ value.

In this description in terms of torsion angles, the "propeller" like forms have all ϕ_i values alike (modulo π) (the other forms being called "nonhelical" ones), and the enantiomer of a given conformation (ϕ_1, ϕ_2, ϕ_3) is ($-\phi_1, -\phi_2, -\phi_3$), both having a pseudo C_3 symmetry.

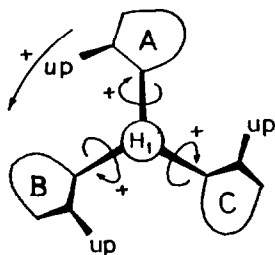
Thus, one enantiomer is not obtained by changing the signs corresponding to all elements of chirality, as Mislow proposed² (see Figure 1). Moreover, as Figure 1 clearly shows, the three elements require an external reference for the determination of the sign. Other approaches for describing this kind of isomerism are equally valid, as pointed out by Mislow,² the choice depending on each particular work. In our case, we are of the opinion that the torsion angle approach, as used by Dunitz *et al.* for the description of interconversion paths between isomers,⁴ is easier to handle and to understand.

The TMBM molecule, with three identical linked rings that have no internal C_2 symmetry axis, has eight possible isomers with propeller conformation represented in Figure 2. They are characterized by the torsion angles (modulo 2π): $A_3 \equiv (\phi, \phi, \phi)$, to which corresponds $B_3 \equiv (\phi \pm \pi, \phi \pm \pi, \phi \pm \pi)$ by x-planar chirality transformation, and, by a, b or c-planar transformations, $A_2B \equiv (\phi, \phi, \phi \pm \pi)$ or $AB_2 \equiv (\phi, \phi \pm \pi, \phi \pm \pi)$, plus their enantiomeric forms changing the helicity, that is, the sign of ϕ .

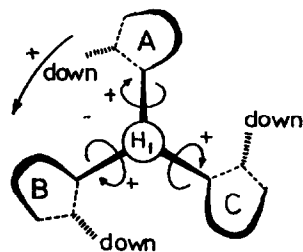
Fig. 1. Mislow's notation in the case of the TMBM molecule and the problem of enantiomerism



a) A TMBM molecule in the $(-+-)x$ conformation, as seen from H(1), according to Mislow. The sense ABC defines the first sign; x corresponds to all 2-methyl substituents on the same side of the N(j1) plane; the second sign means that they are on the H(1) side; the third sign stands for anticlockwise rotation of all three fused rings from the zero position (when perpendicular to the N(j1)'s plane).



b) The enantiomer of the molecule shown in a). It can be seen that the senses of rotation are opposite; the three rings are still above the N(j1)'s plane and on the same side as H(1); finally, the rotation of the three fused rings about C(1)-N(j1) bonds is the opposite as in a). Thus, it must be described as $(+++)$ x.



c) The same as a) but in the conformation described by Mislow as the enantiomer, with all signs reversed, *i.e.* $(+-+)$ x.

The crystals we have studied contain examples of A_3 , \bar{A}_3 , A_2B and $\bar{A}_2\bar{B}$, grouped in two structures: $A_3.\bar{A}_3$ and $A_3.\bar{A}_2\bar{B}$. We have verified that the enantiomer $\bar{A}_3.A_2B$ is crystallographically isomorphous to $A_3.\bar{A}_2\bar{B}$. We have not found samples corresponding to the other four forms.

Interconversion paths between isomers. Stereoisomerization between three bladed propeller forms of a molecule has also been studied by Mislow *et al.*¹⁻³ Leaving aside the inversion mechanism along the C(1)-H(1) line, not possible in the case of TMBM, these interconversion paths are interpreted by the Kurland "flip" mechanisms,⁵ where zero, one, two or the three rings

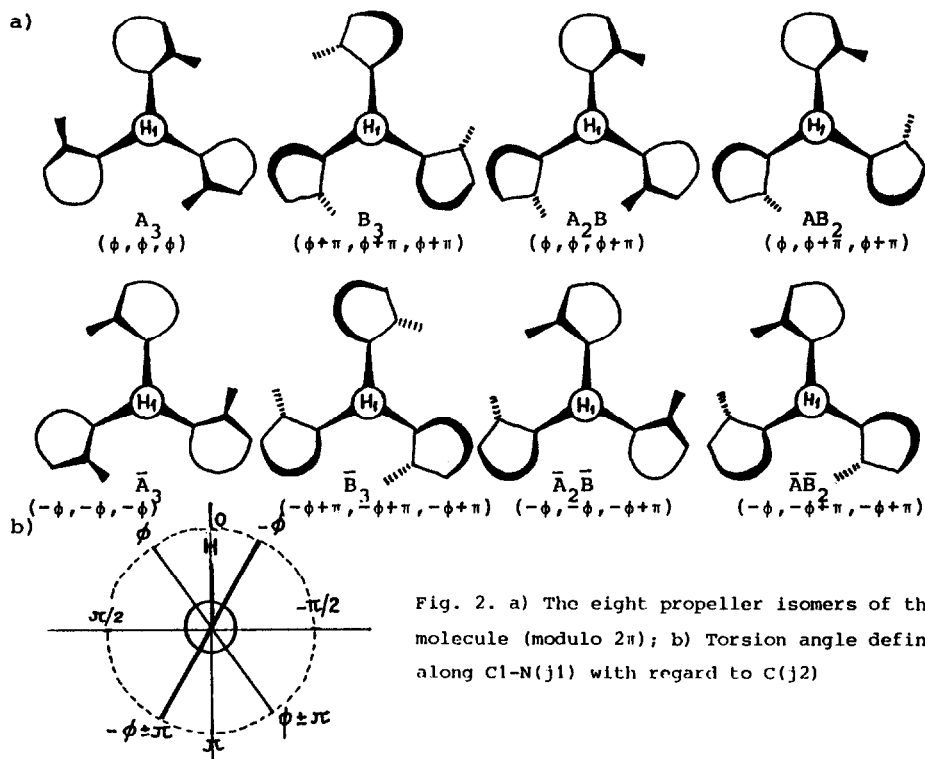


Fig. 2. a) The eight propeller isomers of the TBM molecule (modulo 2π); b) Torsion angle definition along C1-N(j1) with regard to C(j2)

rotate through a torsion value of 0 or π , while the other rings go through $\pm\pi/2$. In both, 0-ring flip and 3-ring flip, the relative sense of rotation of the three rings is the same, while in 1- or 2-ring flip, two rings rotate in a sense and the other in the reverse. In all flips the helicity changes. The rotation of one ring is geared with the remaining ones, resulting in a coupling in their movements which has been called "correlated rotations". The presence of steric hindrance make some of the flips more likely to occur than others.

Dunitz *et al.*^{4,6} have approached the study of these interconversion paths by the Structure-Correlation method.^{7,8} From the geometries found in a large number of structures in the solid state, they developed conformational maps which represent the low energy portions of the reaction coordinate profile. In the case of triphenylphosphine oxides, they result in an approximate two-ring flip path.

As rotation is a periodic phenomenon, the conformational maps of three bladed propellers could be discussed with the same model as that employed for

crystal structures, using the torsion angles ϕ instead of atomic coordinates. The ϕ_i torsion angles ($i = 1, 2, 3$) follow a clockwise sequence, as seen from the top of the central atom. When referred to a central sp^3 frame, with local C_{3v} symmetry, this symmetry provides the equivalent conformations set, which, in this case, corresponds to those described by the Symmetry Space Group $R32$ (D_3^7 , no 155 of reference 9), both symmetry and positions referred to the conformational map, not to the actual molecular geometry. Since in TMBM molecules the blades (the benzimidazole rings) have not internal C_2 symmetry along the bond of rotation, $C(1)-N(j1)$, the "translations" with π components, corresponding to the rotor group, have to be eliminated, leaving a formal unit cell rhombohedral with axis 2π in length. In the better suited hexagonal axis description, the torsion angles ϕ_i are transformed into hexagonal coordinates given by:

$$3x_H = 2\phi_1 - \phi_2 - \phi_3, \quad 3y_H = \phi_1 + \phi_2 - 2\phi_3, \quad 3z_H = \phi_1 + \phi_2 + \phi_3$$

(all in rad. or deg., modulo 2π or 360° , or in fractions of axis, when divided by their modulo, see Fig. 3).

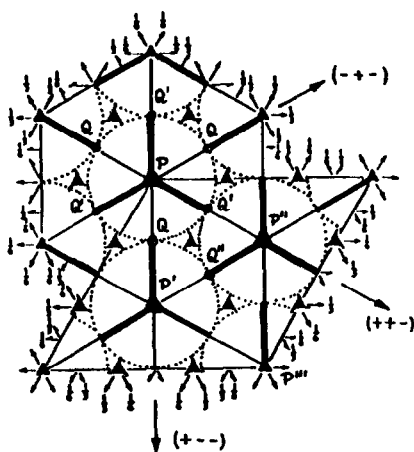


Fig. 3. Representation of the symmetry elements in the conformational map, as seen perpendicular to the threefold rotation axis. Arrows with signs stand for the signs of the ϕ_1 , ϕ_2 and ϕ_3 rotations respectively. (+++) is along OZ^+ . Symmetry operations are, in fractional coordinates, $\pm\{(0,0,0), (1/3, 2/3, 2/3), (2/3, 1/3, 1/3)\}$ as R lattice translations, $\{(x,y,z), (\bar{y}, x-y, z), (y-x, \bar{x}, z)\}$ due to the 3fold axis at $(0,0,0)$ and $\{(y, x, \bar{z}), (\bar{x}, y-x, \bar{z}), (x-y, \bar{y}, \bar{z})\}$ related to the previous one by the 2fold axis along either OX or OY. The helical forms are situated along the lines parallel to the OZ axis and passing through points marked as Q, P and symmetry related like Q', Q'', P', P" and so on.

It is worth to notice that enantiomeric geometries are related by two-fold axis in the conformational map: $(x, y, z) \longrightarrow (\bar{x}, y-x, \bar{z})$. In this representation, the eight helical isomers have the following coordinates (plus the enantiomeric ones among all the equivalent conformations related by symmetry):

Form	Angles (rad)	Fractional coor. ($z=\phi/2\pi$)	Fractional with $\phi = 45^\circ$
A_3	$0, 0, \phi$	$0, 0, z$	$0, 0, 1/8$
B_3	$0, 0, \phi-\pi$	$0, 0, z-1/2$	$0, 0, -3/8$
A_2B	$\pi/3, 2\pi/3, \phi-\pi/3$	$1/6, 1/3, z-1/6$	$1/6, 1/3, -1/24$
AB_2	$2\pi/3, \pi/3, \phi-2\pi/3$	$1/3, 1/6, z-1/3$	$1/3, 1/6, -5/24$

They are represented along the two independent lines, through P and Q (see, Fig. 3) on Fig. 4. Non helical forms, those with ϕ_{\perp} with different values (modulo π), such as $A_2\bar{A}$, $B_2\bar{B}$, $A_2\bar{B}$, $B_2\bar{A}$, $\bar{A}\bar{A}\bar{B}$, $\bar{B}\bar{B}\bar{A}$, $\bar{A}\bar{A}\bar{B}$, $\bar{B}\bar{B}\bar{A}$, and their enantiomers, do not have simple map positions.

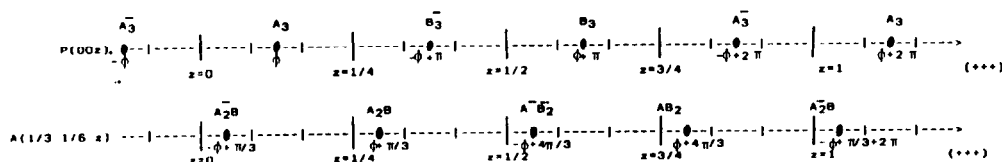


Fig. 4. Distribution of helical forms along the OZ line and through the parallel one through Q. Along these parallel lines, through P' and P", we have the same distribution of forms as that through P, but translated by $\pm 1/3$ respectively. The same relation holds for those lines through Q' and Q", with regard to the line through Q.

In the TMBM molecule, and among what are probably the most stable forms (A_3 , A_2B , \bar{A}_3 , $\bar{A}_2\bar{B}$), the isomerization may be produced along the following paths (and those symmetry related, see Fig. 5):

i) $A_3(\phi, \phi, \phi) \xrightleftharpoons{+++} \bar{A}_3(\bar{\phi}, \bar{\phi}, \bar{\phi})$. A three-ring flip (3RF) way, through the $(0,0,0)$ transition point (TS), hindered by the three H(j7) atoms and, to a less extent, by the methyl (j8) groups. This flip is stopped, in both senses, by the bumping of the methyl groups against the phenyl rings and by the H(j7) atoms against the imidazole rings.

ii) $A_3(\phi, \phi, \phi) \xrightleftharpoons{++-} \bar{A}_2\bar{B}(\bar{\phi}, \bar{\phi}, \bar{\phi}+\pi)$ or $\bar{A}_3(\bar{\phi}, \bar{\phi}, \bar{\phi}) \xrightleftharpoons{+-+} A_2B(\phi, \phi, \phi-\pi)$ in 2RF ways, through the $(0,0, \pm\pi/2)$ TS's. These ways are hindered still by two H(j7) atoms, but they are geared by a methyl group against the proton in the rotating blade, and by one H(j7) pulling the phenyl ring of that blade.

Thus, this path is favored with regard to the first way. This second way is stopped in analogous form as in i).

iii) $A_2B(\phi, \phi, \phi - \pi) \xrightleftharpoons{+++} \bar{A}_2\bar{B}(\bar{\phi}, \bar{\phi}, \bar{\phi} - \pi)$ or $\bar{A}_2\bar{B}(\bar{\phi}, \bar{\phi}, \bar{\phi} + \pi) \xrightleftharpoons{+++} A_2B(\phi, \phi, \phi + \pi)$ in 3RF path, through $(0, 0, \pi)$ as TS. It is hindered by a methyl group against two H(j7) and it is stopped in the usual way.

iv) $A_2B(\phi, \phi, \phi + \pi) \xrightleftharpoons{++-} \bar{A}_3(\bar{\phi}, \bar{\phi}, \bar{\phi} + 2\pi)$ or $\bar{A}_2\bar{B}(\bar{\phi}, \bar{\phi}, \bar{\phi} - \pi) \xrightleftharpoons{++-} A_3(\phi, \phi, \phi - 2\pi)$ similar to the second path.

Of course, the actual path does not need to follow the straight lines drawn in Fig. 5. Close circuits may be followed through conformations on P lines, at $z = 0$ or ± 1 levels. They are connected through conformations along lines at P', Q'' and P'' (see Figs. 3 and 5).

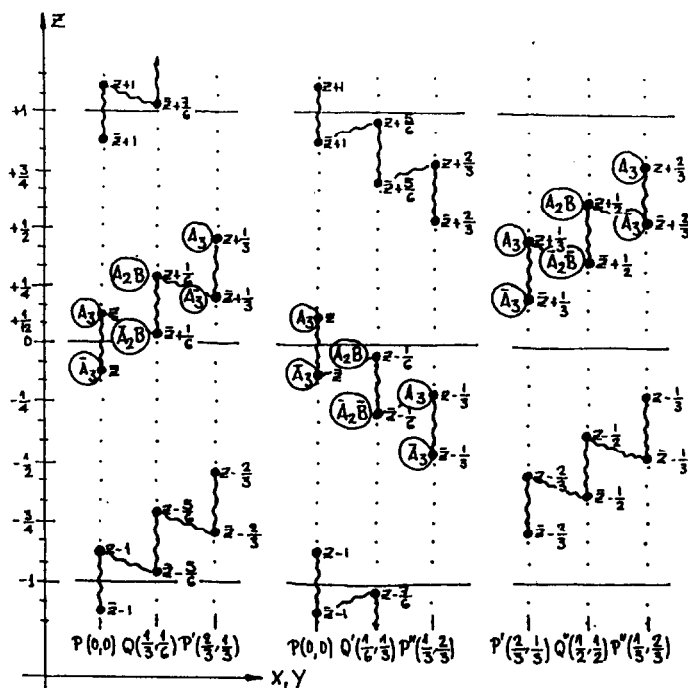
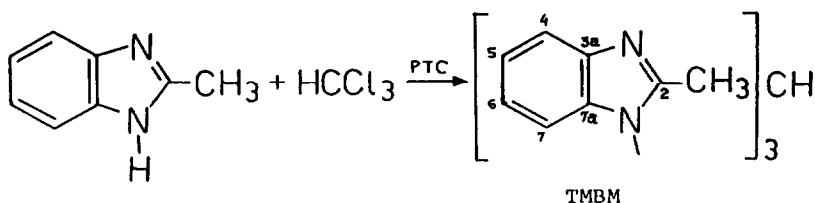


Fig. 5. Joint distribution of the forms most likely to occur at the lines parallel to OZ through: a) P, Q and P', along $(+++)/(---)$ and $(+-)/(-+-)$ directions. b) P, Q' and P'', along $(+++)/(---)$ and $(+-)/(-+-)$ directions. c) P', Q'' and P'', along $(+++)/(---)$ and $(+-)/(-+-)$ directions. The figure shows the 3RF and 2RF interconversion paths (wavy segments).

RESULTS AND DISCUSSION

Our interest in polyazolylmethanes,¹⁰⁻¹⁹ encouraged us to synthesize a derivative in which resolution and racemization experiments together with dynamic n.m.r. (DNMR) studies could be carried out. After an unsuccessful attempt with tris-(3',5'-dimethylpyrazol-1'-yl)methane,¹⁹ we decided to prepare tris-(2'-methylbenzimidazol-1'-yl)methane, TMBM. This compound was chosen for two main reasons: the lack of isomerism of position, since both nitrogens are equivalent, and a reasonable steric crowding enough for both enantiomers to be stable at room temperature but, at the same time, allowing the DNMR studies.

Chemistry.- TMBM was prepared using the general synthetic procedure for trisazolylmethanes.¹⁴



Characterization of TMBM.- The compound was characterized by its ¹H and ¹³C n.m.r. spectra (Table 1). All signals were assigned unambiguously by means of 2D experiments, both ¹H-¹H and ¹H-¹³C.

If both enantiomers of TMBM are separated by a racemization barrier high enough for the process to be "slow" in the n.m.r. time scale, addition of a chiral reagent should split some of its signals. A first attempt using Eu(tfc)₃ failed (only shifting and broadening of all signals were observed). Better results were obtained using Pirkle's alcohol, R(-)-2,2,2-trifluoro-1-(9-anthryl)ethanol (for details, see Experimental Part). When adding Pirkle's alcohol to a CDCl₃ solution of TMBM, the signals of the 2-methyl group and of the sp³ C-H, split off into two singlets of the same intensity. For a larger concentration of the chiral alcohol, the multiplet of H4 proton also splits. Thus, TMBM is a mixture of two slowly interconverting enantiomers.

A NOESY experiment (see Experimental Part) on TMBM clearly shows a correlation between the methyl and methine protons and a much less intense spot corresponding to the interaction between H7 and the methine proton. This shows that in solution, the averaged conformation of TMBM has the methyl group on the same side than the CH(1), but that minor conformations exist where the benzimidazole H7 and the CH(1) are on the same side, that is, a mixture of A₃ and A₂B (Fig. 2) with the former predominating.

Table 1. Chemical shifts (δ) and coupling constants (Hz) of TMBM

Solvent	H4	H5	H6	H7	CH (1)	CH ₃
CDCl ₃	7.80	7.29	7.02	6.10	8.57	2.35
	(J ₄₅ =8.2) (J ₅₆ =7.5) (J ₄₆ =1.0) (J ₆₇ =8.2) (J ₅₇ =1.1)					
DMSO-d ₆	7.73	7.23	6.96	5.84	9.12	2.34
CD ₃ OD	7.94	7.50	7.18	6.09	9.23	2.60

Solvent	C2	C3a	C4	C5	C6	C7	C7a	CH	CH ₃
CDCl ₃	150.1	142.3	120.4	123.7	124.7	109.6	133.4	74.5	14.5
	² J=6.5	³ J=5.9	¹ J=163.2	¹ J=161.7	¹ J=162.8	¹ J=164.7	³ J=8.0	¹ J=166.0	¹ J=129.7
		³ J=8.9	³ J=8.0	³ J=7.6	³ J=7.8	³ J=8.4	³ J=8.0		
CD ₃ OD	153.5	143.2	121.1	125.5	126.1	111.5	134.8	76.4 ^a	14.3
Solid State	151.5 ^b	144.3 ^c	117.5 ^c	121.3 ^b	127.8 ^b	109.5 ^c	132.6 ^d	74.3 ^d	13.7 ^b
	151.0 ^c	142.3 ^c	118.1 ^c	123.4 ^c	126.0 ^c	111.4 ^b			15.2 ^c
		141.7 ^b	119.7 ^b	124.8 ^c					
		140.7 ^b	120.5 ^b						

^a At 223 K this signal splits into 76.2 (strong) and 76.5 (small); ^b Strong; ^c Small; ^d Broad signal.

Besides, the ¹³C CP/MAS spectrum of racemic TMBM in the solid state (Table 1) was very complex. Some signals were broad, some splitted into two and even into four lines, indicating the existence in the crystal of several conformations or, at least, of several positions for each benzimidazole ring in one TMBM molecule.

Resolution of TMBM.- Resolution of TMBM was performed by chromatography on microcrystalline cellulose triacetate (MCT)²⁰ a method which we had already used in polyazolyalkanes (separation of classical enantiomers having a chiral central sp³ carbon atom).¹⁷ There is no example in the literature of resolution of helical enantiomers using MCT.

With the apparatus and conditions described in the experimental part, two fractions of TMBM were obtained. The first eluted fraction had a rotatory power $[\alpha]_{436}^{25} = 334$ in 95% ethanol and it was enantiomerically pure, at least in the presence of Pirkle's alcohol only one methyl signal was observed (less than 3% of the other enantiomer). The second fraction contained the (-)TMBM (same absolute value of $[\alpha]$). Suitable crystals were obtained from the racemic and from both enantiomers (solvent, water-ethanol).

X-Ray Crystallography

Structure and Constitution.— The main characteristics of the molecular geometries are presented in table 2, where 1 is the enantiomer C^+ and 2 is the racemic $C^{+/-}$.

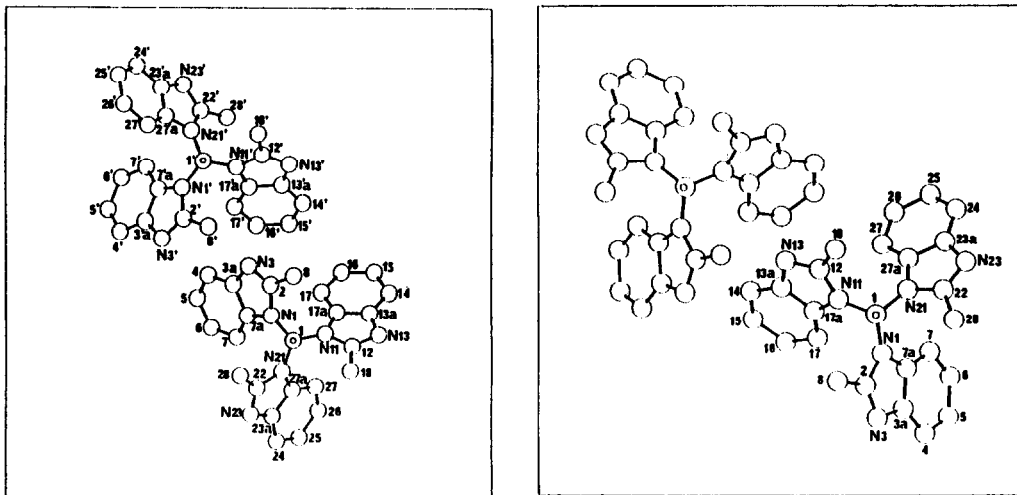


Table 2 . Selected geometrical parameters (Å, °)

Molecule	1		2	Molecule	1		2
	Undashed	Dashed			Undashed	Dashed	
C1-M1	1.452(6)	1.467(8)	1.441(5)	C1-M11	1.437(8)	1.441(8)	1.458(4)
C1-M21	1.436(6)	1.460(8)	1.455(4)	C1-H1	0.94(6)	0.97(5)	1.00(3)
N1-C2	1.381(8)	1.378(8)	1.396(5)	N1-C7A	1.392(8)	1.384(8)	1.401(4)
C2-M3	1.289(9)	1.315(9)	1.294(5)	C2-C8	1.492(11)	1.467(10)	1.481(6)
N3-C3A	1.388(9)	1.371(9)	1.390(4)	C3A-C7A	1.408(9)	1.407(9)	1.404(5)
N11-C12	1.387(9)	1.379(9)	1.374(5)	N11-C17A	1.396(8)	1.412(8)	1.405(4)
C12-M13	1.300(10)	1.301(9)	1.314(4)	C12-C18	1.495(11)	1.486(11)	1.474(6)
N13-C13A	1.376(9)	1.388(9)	1.387(5)	C13A-C17A	1.384(9)	1.385(9)	1.402(5)
N21-C22	1.397(8)	1.384(8)	1.389(4)	N21-C27A	1.394(8)	1.388(8)	1.404(4)
C22-M23	1.299(8)	1.299(9)	1.299(5)	C22-C28	1.473(11)	1.497(10)	1.490(6)
N23-C23A	1.380(8)	1.381(9)	1.393(4)	C23A-C27A	1.402(9)	1.376(9)	1.398(4)
N21-C1-H1	108(4)	108(3)	106(2)	N11-C1-H1	108(4)	106(3)	107(2)
N1-C1-H1	105(4)	108(3)	108(2)	N11-C1-N21	112.0(3)	113.0(5)	111.5(3)
N1-C1-N21	112.3(3)	110.9(5)	111.7(3)	N1-C1-M11	111.8(3)	111.1(5)	112.2(3)
C1-M1-C7A	128.9(5)	131.1(5)	130.7(3)	C1-M1-C2	123.6(5)	121.2(5)	122.4(3)
C2-M1-C7A	107.5(5)	107.7(5)	106.6(3)	N1-C2-C8	122.1(6)	122.0(6)	122.3(4)
N1-C2-M3	112.3(6)	110.9(6)	111.9(3)	N3-C2-C8	125.6(6)	127.0(6)	125.8(4)
C2-N3-C3A	106.4(6)	107.2(5)	107.0(3)	N3-C3A-C7A	110.1(6)	109.5(6)	109.7(3)
N1-C7A-C3A	103.9(5)	104.8(5)	104.8(3)	C1-M11-C17A	130.8(4)	130.6(5)	129.3(3)
C1-M11-C12	123.1(5)	122.5(5)	123.1(3)	C12-M11-C17A	105.7(5)	106.8(5)	107.5(3)
N11-C12-C18	122.7(7)	122.7(6)	123.4(3)	N11-C12-M13	112.5(6)	111.9(6)	112.3(3)
N13-C12-C18	124.8(7)	125.4(6)	124.3(3)	C12-M13-C13A	106.1(8)	106.5(6)	105.4(3)
N13-C13A-C17A	110.4(6)	110.4(6)	111.1(3)	N11-C17A-C13A	105.4(5)	104.4(5)	103.6(3)
C1-M21-C27A	130.3(5)	120.1(5)	130.4(2)	C1-M21-C22	124.1(5)	132.8(5)	122.5(3)
C22-M21-C27A	105.5(5)	107.1(5)	106.8(2)	N21-C22-C28	121.6(6)	125.5(6)	122.5(3)
N21-C22-M23	113.5(6)	111.2(6)	112.3(3)	N23-C22-C28	124.9(6)	123.3(6)	125.2(3)
C22-M23-C23A	105.2(5)	106.4(6)	106.1(3)	N23-C23A-C27A	110.9(5)	110.5(6)	110.4(3)
N21-C27A-C23A	104.9(5)	104.8(5)	104.4(3)				
H1-C1-M1-C2	43(4)	-44(3)	+/-38(2)	H1-C1-M11-C12	40(4)	-36(3)	+/-37(2)
H1-C1-M21-C22	41(4)	139(3)	+/-42(2)				

The structure of $C^{+/-}$ is formed by two enantiomeric types of TMBM, which surround a six-membered ring system of water molecules in a centrosymme-

tric arrangement. The independent TMBM molecule has an approximate C_3 symmetry, with C-N distances ranging from 1.441(5) to 1.458(4) Å, and H-C-N angles between 107(2) and 108(3)°.

In the C^+ structure, there are two crystallographically independent TMBM molecules which are chemically isomeric (see below), and seven water molecules. The central part of both types of molecules have an approximate C_{3v} frame, with C-N distances from 1.436(6) to 1.467(8) Å and H-C-N angles from 105(4) to 108(4)°. It is worth to notice the change in the angular values $C1'-N21'-C27A' = 120.1(5)^\circ$ vs. $C1'-N21'-C22' = 132.8(5)^\circ$, while in the other heterocycles the equivalent angular values are such as $C-N-CA > C-N-C$, even in compound 2.

Conformational chirality.— No attempts to determine the absolute chirality of C^+ have been done. The relative conformation of the TMBM molecules, in both structures, has been analyzed in terms of the torsion angles $\phi_i = H1-C1-Nj1-Cj2$ ($j = 0, 1, 2$) (see Table 2).

The independent molecules in $C^{+/-}$, and the undashed one in C^+ , have a chiral propeller conformation of approximate C_3 symmetry. The values of the ϕ_i torsion angles, all near $\pm 40^\circ$, situate that conformation in the so-called three-fold axis cluster,⁶ formed by the most frequent conformations found in the triphenylphosphine oxides and related molecules.

In C^+ there is another independent TMBM molecule, isomer of the first one, with two ϕ torsion angles near -40° and the third one 180° apart.

The Cambridge Structural Database,²¹ was searched for molecules capable of reaching a C_3 propeller conformation and with blades without C_2 internal symmetry. We used connectivity and names, excluding metal containing compounds, triphenylphosphine derivatives and compounds with the blades interconnected in some way,²² finally we were left with:

i) Tris-(3',5'-dimethylpyrazol-1'-yl)methane²³ (see also ref. 19). It is a $P2_1/n$ crystal, with four crystallographic independent molecules. The H-C-N-C torsion angles have values, for each molecule, of (38.1,59.0,-160.9), (37.9,61.2,-161.6), (27.6,57.3,-160.4) and (26.8,66.0,-162.7°) which correspond to a distorted $A_2B \equiv (\phi, \phi, \phi - \pi)$ conformation.

ii) Tri-*o*-tolyl-phosphine oxide, -phosphine-sulphide and -phosphine-selenide.²⁴ All compounds crystallize in centrosymmetric structures with two, three, two and one crystallographically independent molecules, respectively. The torsion angles are: a) $-P-C-C$ (Me linked): (39.4,45.5,43.2) and (35.9,47.0,41.9), thus it is an A_3 form. b) $O-P-C-C$ (Me linked): (50.7,43.0,44.4), (44.6,51.9,42.2) and (49.9,48.9,38.0), again an A_3 conformation. c) $S-P-C-C$ (Me linked): (52.7,59.3,-172.9) and (56.6,56.5,-162.9) in an approximate A_2B conformation. d) $Se-P-C-C$ (Me linked): (53.9,59.5,-167.7°) as in c).

iii) Tri-*m*-tolyl-phosphine, -phosphine-sulphide and phosphine-selenide.²⁵ All of them crystallize in the Pbc_a group, with just one independent molecule and with corresponding torsion angles of: a) :-P-C-C (nearest to the substituent): (36.3, 46.0, -128.0), which belongs to an A₂B form. b) S-P-C-C (nearest to the substituent): (15.2, -120.6, -155.0), which corresponds to an approximate AB₂ ≡ (φ, φ-π, φ-π) but quite near to (0, -2π/3, π). c) Se-P-C-C (nearest to the substituent): (13.8, -119.1, -155.9°), like in b).

iv) There is a modification of iii a), tris-*m*-trifluoromethylphenyl-phosphine-selenide,²⁶ which maintains the Pbc_a symmetry group. The only independent molecule has torsion angles of (-22.2, 5.9, 96.9°), in this case near (0, 0, π/2).

In conclusion, concerning the molecular structure of TMBM we have found two kinds of conformations, namely Λ₃ (φ, φ, φ) (φ_i = ±40°) and $\bar{\Lambda}_2\bar{B}$ (φ, φ, φ-π) (φ_i = ±40°), both previously found, but never for the same compound.

The near C₃ symmetry of the racemic, C^{+/-}, does not seem to be in agreement with the ¹³C n.m.r. spectrum of the solid sample (Table 1) which appears most consistent with an $\bar{A}_2\bar{B}$ structure. The observed splitting of signals does not correspond to an Λ₃/ $\bar{\Lambda}_3$ mixture, since the signal that splits at low temperature is that of C(1) and not the methyl nor the aromatic carbons.

Packing.- The molecules of TMBM pack in the crystals through a remarkable network of hydrogen bonds (see Figs. 6 and 7) involving all the water molecules and the acceptor nitrogen atoms, N(j3). In compound 1 ≡ C⁺, the water molecules form chains, along the *c* axis, with a six-membered heterodromic ring²⁷ linked by an isolated water molecule. In compound 2 ≡ C^{+/-}, no such

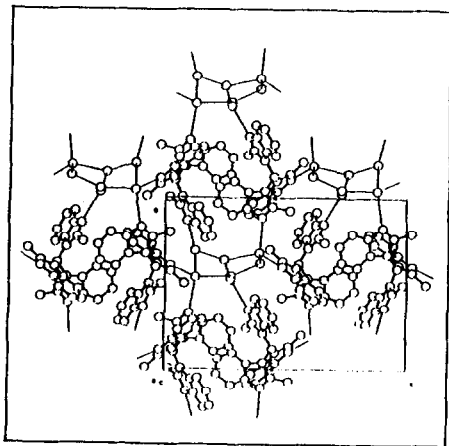


Fig. 6. The packing of 1 = C⁺

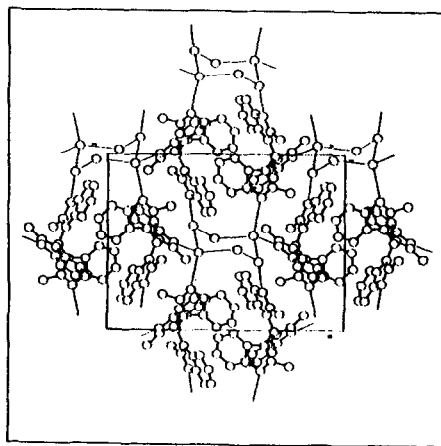


Fig. 7. The packing of 2 = C^{+/-}

water molecule is present and the rings are isolated. The geometry of these networks is given in Tables 3 and 4. In the case of 1, the water ring has an envelope conformation, flapping at O(4), with three types of water molecules: those involved in four interactions, O(1) and O(21), that involved just in two interactions, O(3), and the remaining ones involved in three hydrogen-bonds. In compound 2, there are two water molecules, with two, three and four contacts [O(3), O(2) and O(1), respectively, and symmetry related] forming a six-membered ring with chair conformation. The ring is centered in a crystallographic inversion point, the internal hydrogen interactions being also heterodromic.

Table 3. Packing characteristics ($\text{\AA},^\circ$):1

a.- Water chain			
O1...O5	2.952(9)	O1...O4	2.808(10)
O6...O5	2.741(12)	O3...O5	2.711(11)
O3...O2	2.941(10)	O2...O7	2.895(13)
O7...O4	3.038(15)	O6...O71	2.826(14)
O4...O1...O5	104.6(3)	O1...O5...O6	111.3(3)
O1...O5...O3	129.4(4)	O3...O5...O6	116.4(4)
O5...O3...O2	116.6(3)	O3...O2...O7	108.4(3)
O2...O7...O4	115.1(4)	O7...O4...O1	102.9(4)
O5...O6...O71	140.1(5)	O2...O7...O611	104.3(4)
O4...O7...O611	139.6(5)		
O1...O5...O3...O2	-8.9(7)	O5...O3...O2...O7	-1.7(5)
O3...O2...O7...O4	43.3(5)	O2...O7...O4...O1	-77.3(5)
O7...O4...O1...O5	57.9(4)	O4...O1...O5...O3	-23.4(6)
b.- Other hydrogen bonds			
O1...N3111	2.884(8)	O1...N131v	2.812(8)
O2...N3'v	2.889(8)	O2...N13'11	2.858(9)
O4...N23v1	3.052(11)	O6...N23'v11	2.860(11)
O1-H1A	0.92(13)	O1-H1B	1.05(13)
O2-H2A	0.99(9)	O2-H2B	1.04(19)
O3-H3A	1.29(8)	O3-H3B	0.96(9)
O4-H4A	0.99(30)	O4-H4B	0.97(21)
O5-H5A	0.99(-)	O5-H5B	0.99(-)
O6-H6A	1.01(-)	O6-H6B	1.18(-)
O7-H7A	0.99(-)	O7-H7B	1.03(-)
H1A...N3111	2.06(14)	O1-H1A...N3111	149(11)
H1B...N131v	1.66(13)	O1-H1B...N131v	149(11)
H2A...N23'v1	1.68(8)	O2-H2A...N23'v11	149(7)
H2B...N3'v	1.91(19)	O2-H2B...N3'v	155(14)
H3A...O5111	1.87(8)	O3-H3A...O5111	140(6)
H3B...O2111	1.98(9)	O3-H3B...O2111	175(7)
H4A...O1111	2.01(27)	O4-H4A...O1111	136(21)
H4B...N23v1	2.27(21)	O4-H4B...N23v1	138(16)
H5A...O1111	1.96(-)	O5-H5A...O1111	179(-)
H5B...O6111	1.75(-)	O5-H5B...O6111	179(-)
H6A...O71	1.81(-)	O6-H6A...O71	179(-)
H6B...N23'v11	1.92(-)	O6-H6B...N23'v11	134(-)
H7A...O2111	1.91(-)	O7-H7A...O2111	179(-)
H7B...O4111	2.00(-)	O7-H7B...O4111	180(-)

Symmetry code :

i = x, y, 1-z
 iii = x, y, z
 v = 1-x, 1/2+y, -z
 vii = 1-x, -1/2+y, 1-z

ii = x, y, 1-z
 iv = -x, 1/2+y, 1-z
 vi = x, 1+y, z

Table 4. Packing characteristics ($\text{\AA},^\circ$):2

a.- Water ring			
O1...O2	2.805(5)	O1...O3	2.995(7)
O2...O3(1)	2.878(7)		
O1...O2...O3(1)	100.6(2)	O1...O3...O2(1)	116.2(2)
O2...O1...O3	98.3(2)		
O3...O1...O2...O3(1)	-61.2(2)	O2...O1...O3...O2(1)	73.7(2)
O1...O3...O2(1)...O1(1)	-75.1(2)		
b.- Other hydrogen bonds			
O1...N3	2.809(5)	O1...N23(11)	2.888(4)
O2...N13(111)	2.966(5)	O1-H1A	0.91(7)
O1-H1B	0.75(8)	H1A...N3	1.90(7)
H1B...N23(11)	2.13(8)	O1-H1A...N3	176(6)
O1-H1B...N23(11)	172(7)		

Symmetry code:

i = -x, 1-y, 1-z
 iii = 1-x, y+1/2, 1/2-z

ii = 1-x, y-1/2, 1/2-z

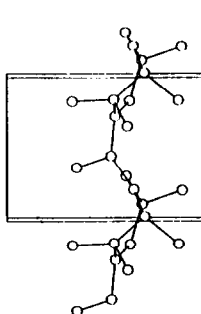


Fig. 8

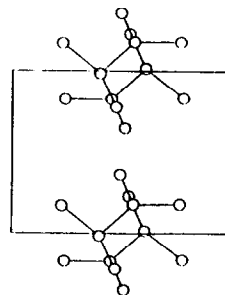


Fig. 9

Figs. 8 and 9. The arrangement of the water molecules; seven, forming chains all along the crystal, in 1: $A_3 \cdot \bar{A}_2 \cdot \bar{B} \cdot 7H_2O$; and in centrosymmetric chair rings in 2: $A_3 \cdot \bar{A}_3 \cdot 6H_2O$.

There are nine possible ways to arrange six water molecules in a hydrogen-bonding network forming a pseudo six-membered ring (Fig. 10).

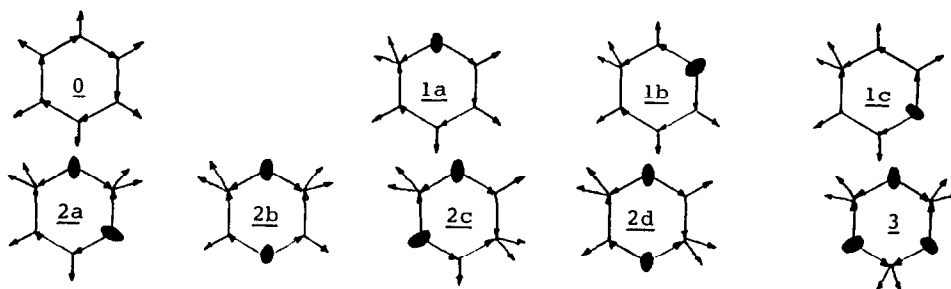
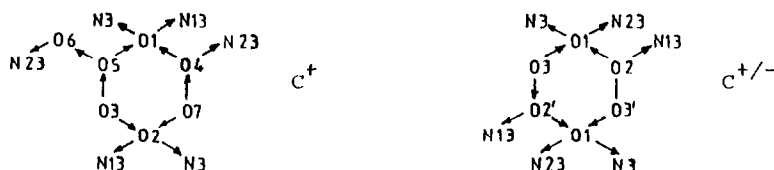


Fig. 10. The nine possible ways of arranging six water molecules in a ring with different donor-acceptor situations.

In TMBM structures, C^+ presents a 2c type network while that of $C^{+/-}$ is 2d type. Both are almost the same, except that the water molecules corresponding to O5 and O3 in C^+ have interchanged, in $C^{+/-}$, with O3-O2'.



Figs. 11 and 12 compare, for $C^{+/-}$ and C^+ , the extent of the cavities holding the water molecules, the similarities of the inclusion systems to form the crystal structure and, also, the differences due to the seventh water molecule and the π - ϕ ring twist. The channel in C^+ becomes cavities in $C^{+/-}$, both bound by the acceptors N's of the TMBM. For unit cell volumes of 2425.4 and 2482.7 \AA^3 for $C^{+/-}$ and C^+ , respectively, the TMBM molecules occupy 1401.6 and 1409.0 \AA^3 (the difference is due to the different conformations), while adding the smoothing of the 1.6 \AA rolling sphere these volumes become 2012.8 and 1983.1 \AA^3 (Fig. 11b and 12b).

Fig. 11:

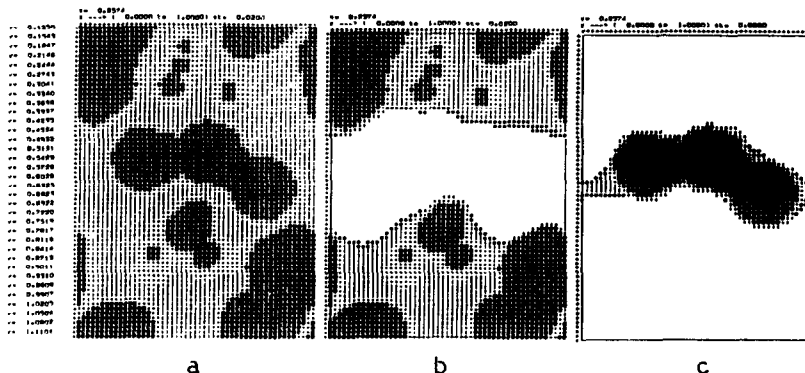
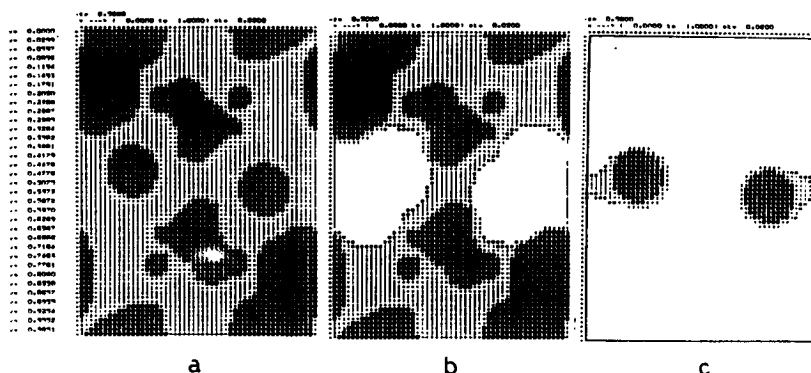


Fig. 12:



Figs. 11 and 12. Sections Y,Z ($X = \text{Constant}$) across the centroids of the water ring systems for $C^{+/-}$ (Fig. 11) and C^+ (Fig. 12), showing the holes (b) inside which are included the water molecules (c), to give the hydrated structure (a). A 0.2 \AA grid was used for the drawings and a rolling sphere of 1.60 \AA was used for smoothly filling the molecular clefts. Dark field indicate atomic van der Waals sections, surrounded by surface points (full account of the method will be published elsewhere).

Dynamic Studies

Racemization.— The racemization experiment was carried out as already described (see Experimental Part) at 343.15 K using 1,2-dimethoxyethane as solvent. The results correspond to a first-order kinetics with $t_{1/2}(\text{min}) = 1157 \pm 2$, $k_{\text{rot}}(\text{sec}^{-1}) = 4.99 \pm 0.01 \cdot 10^{-6}$, and $\Delta G_{343}^{\ddagger} = 28.47 \pm 0.04 \text{ kcal} \cdot \text{mol}^{-1}$.

^1H n.m.r. study at low temperature (DNMR).— When a deuteromethanolic solution of racemic TMBM is cooled down at 175 K , the signals of a 86%-14% ($K_{\text{eq}} = 6.1$) mixture of A_3 and $\bar{A}_2\bar{B}$ isomers are observed. An analysis of the six spectra obtained between 298 and 175 K allows to determine the interconversion barrier between both isomers, $\Delta G^{\ddagger}(A_3 \rightarrow \bar{A}_2\bar{B}) = 9.8 \pm 0.1 \text{ kcal} \cdot \text{mol}^{-1}$. The analysis, carried out by Professor Jan Sandström (University of Lund, Sweden) used both the methine proton (two signals) and the methyl group (four signals). The calculated value for the activation energy is the same using one or the other signal.

The spectrum at 175 K leaves no doubt of the structure of the minor isomer; whereas the major one has a C_{3v} symmetry (CH_3 at $\delta 2.72$, CH at $\delta 9.39$), the minor one shows the methine proton at 9.67 and the 2-methyl substituent as three broad signals of the same intensity at $\delta 2.93$, 2.7 (under the signal belonging to A_3) and 2.02 . The last signal belongs to the methyl "down" of the $\bar{A}_2\bar{B}$ isomer (Fig. 2) shielded by the ring currents of the benzene rings. The methyl groups "up" (\bar{A}_2 part) are anisochronous since this isomer lacks all symmetry elements. Isochrony of methyl "up" signals would correspond, either to the $(0,0,\pi)$ conformation (C_s symmetry) or to a rapid $\bar{A}_2\bar{B} \rightleftharpoons A_2B$

interconversion through it. Both possibilities can be ruled out, since the $(0,0,\pi)$ conformation is just the highest transition state (TS_2) in TMBM dynamics (see later on).

CONCLUSIONS

Assuming some simplifications, we have obtained, for the first time, a complete energy profile for a three-blade propeller of the characteristics of TMBM (sp^3 central atom without inversion and "assymmetric" blades) (Fig. 13).

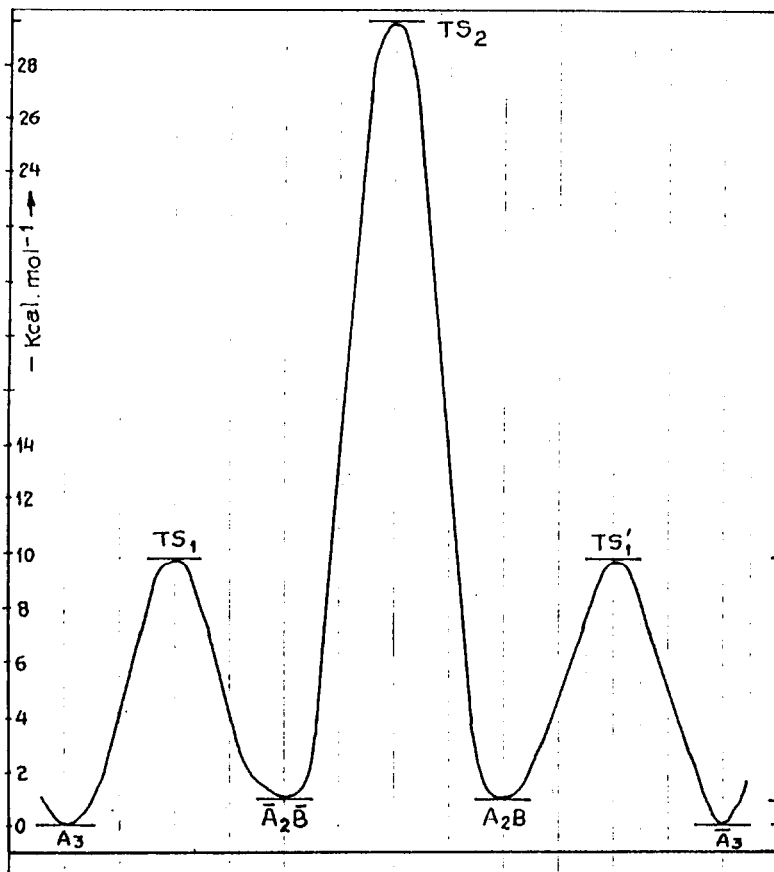


Fig. 13. Energy profile of TMBM interconversions

The difference in energy between both isomers has been estimated from the value of the equilibrium constant ($K_e = 6.1$) determined in methanol at 175 K. Assuming that the equilibrium constant is the same at 343 K, $\Delta G = 1.2$ kcal.mol⁻¹. The barrier through TS_1 resulted also from the DNMR experiment, 9.8 kcal.mol⁻¹, going from the most stable isomer, A_3 to the less stable

one, $\bar{A}_2\bar{B}$. Finally, the barrier through TS_2 ($28.5 \text{ kcal.mol}^{-1}$) was obtained from the racemization experiment.

The profile of Fig. 13 corresponds to Mislow's type graph¹ of Fig. 14.

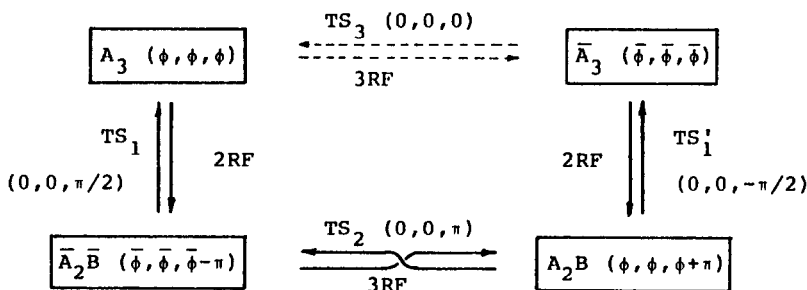


Fig. 14. Reaction graph of TMBM isomerizations

With Figures 13 and 14 it is possible to understand all the observed phenomena of TMBM we have previously reported:

i) Isomers A_3 and A_2B being of similar energy are both found in crystals. There is no energetic reason why $A_2B(\bar{A}_2\bar{B})$ should not be present in the racemic. It seems that two molecules of TMBM, together with solvation water, are necessary to form a stable crystal structure. In the case of the racemic, the solution to this problem is an $A_3 \cdot \bar{A}_3$ mixture, whereas in the case of pure enantiomers, the solution is an $A_3 \cdot \bar{A}_2\bar{B}$ ($\bar{A}_3 \cdot A_2B$) mixture.

ii) The measured rotatory power corresponds to a mixture (about 80%-20%) of \bar{A}_3 and $\bar{A}_2\bar{B}$ isomers (or \bar{A}_3 and A_2B) in rapid equilibrium.

iii) The splitting of 1H n.m.r. signals in the presence of Pirkle's alcohol corresponds to both sides of the graph (Fig. 14) with regard to TS_2 , whereas the splitting at low temperatures corresponds to both sides with regard to TS_1 (TS_1').

iv) Nothing is known about the highest energy path through TS_3 . Examination of CPK models indicate that this is certainly a much higher transition state due to close contacts between H₇ atoms.

v) The non observed isomers, B_3 and AB_2 (\bar{B}_3 and $\bar{A}\bar{B}_2$) correspond to highly strained situations.

vi) The $A_3 \rightarrow \bar{A}_2\bar{B} \rightarrow A_2B \rightarrow \bar{A}_3$ and backwards path can be described as beginning with an oscillation around the A_3 equilibrium position; when these oscillations couple with methyl rotations, and the system has enough energy, a geared rotation of two rings is observed ($A_3 \rightarrow \bar{A}_2\bar{B}$). If much more energy is provided to the system, then a new three ring flip occurs, also in a geared way ($\bar{A}_2\bar{B} \rightarrow A_2B$).

EXPERIMENTAL SECTION

General Experimental Procedures.- Melting points were determined in a capillary tube with a Büchi 530 apparatus and are uncorrected. ^1H n.m.r. (200.13 MHz) and ^{13}C n.m.r. (50.32 MHz) spectra were obtained with Bruker AM-200 (Faculty of Sciences, Université d'Aix-Marseille III, France) and Bruker AC-200 (Faculty of Sciences, UNED, Spain) instruments. Chemical shifts (δ) in ppm and coupling constants (J) in Hz were measured in 10% (w/v) solutions with Me_4Si as internal standard. The ^1H and ^{13}C chemical shifts are accurate to 0.01 and 0.1 ppm, respectively. Coupling constants are accurate to 0.2 Hz for ^1H n.m.r. and 0.5 Hz for the ^{13}C n.m.r. The mass spectrum was recorded on a VG-12-250 spectrometer operating at 70 eV.

Synthesis of Tris-(2'-methylbenzimidazol-1'-yl)methane.- A mixture of 2-methylbenzimidazole, 22.7 mmols, 114 mmols of anhydrous potassium carbonate and 1.2 mmols of tetrabutylammonium bromide was vigorously stirred and refluxed in dry chloroform (30 ml) for 8 h. The mixture was filtered and the residue washed with hot chloroform (3 x 25 ml). The organic solution was evaporated and the crude product purified by column chromatography on silica gel Merck 60 (70-230 mesh, ASTM) with ethyl acetate-methanol (9:1) as eluent, $R_f = 0.19$. Yield, 43%, m.p. 214-5°C (EtOH-H₂O). Mass spectrum, $M^+ = 406$.

Anal. Calcd. for $\text{C}_{25}\text{H}_{22}\text{N}_6 \cdot 3\text{H}_2\text{O}$: C, 65.20; H, 6.13; N, 18.25. Found: C, 66.36; H, 6.51; N, 18.63.

The compound was sublimated, m.p. 118°C (Lit. m.p. 110°C).¹⁴

Anal. Calcd. for $\text{C}_{25}\text{H}_{22}\text{N}_6$: C, 73.87; H, 5.46; N, 20.67. Found: C, 74.17; H, 5.50; N, 20.70.

COSY and NOESY n.m.r. Experiments.- These 2D-experiments were run on the Bruker AM-200 spectrometer according to the following data acquisition parameters: i) for the 2D-COSY experiment, F_1 domain (SI1, 1K; SW1, 958 Hz; D1, 1s), F_2 domain (SI2, 2K; SW2, 1916 Hz), NS, 16; DS, 2. ii) for the 2D-NOESY experiment, F_1 domain (SI1, 1K; SW1, 958 Hz; D1, 1s), F_2 domain (SI2, 2K; SW2, 1916 Hz), NS (number of transients per FID), 96; DS (number of preparatory dummy transients per FID), 2. All the 2D experiments were processed with a sine bell window (WDW1 = WDW2 = S, SSB1 = SSB2 = 0).²⁸

DNMR Experiments.- The ^1H n.m.r. spectra of TMBM were recorded at 298, 220, 200, 190, 180 and 175 K in CD_3OD using the Bruker AC200 instrument. The temperature calibration was performed using the methanol signal and a delay of 15 min was used before registering the n.m.r. spectra at each temperature.

Separation by Liquid Chromatography on Microcrystalline Cellulose Triacetate (MCT).— The technique and apparatus for separation of enantiomers on MCT have been described elsewhere.^{17,29} A solution of 15 mg of racemic TMBM in 4 ml 95% ethanol is injected in one column of 20 cm length with an internal diameter of 2.5 cm; phase, MCT 15-25 microns from Merck; flow rate, 92 ml/h; pressure drop, 1.6 bar; temperature, 20°C. Using 1,3,5-tri-tert-butylbenzene as reference ($V_0 = 14.45$ cm), a LKB 2138 UVICORD S detector ($\lambda = 254$ nm), a 241 MC Perkin Elmer polarimeter ($\lambda = 436$ nm) for the detection of the compounds and after four cyclic passages of the enriched fractions, the (+) enantiomer ($V = 16.90$ cm, $k'(+)$ = 0.29), m.p. 109-11°C and the (-) enantiomer ($V = 18.70$ cm, $k'(-)$ = 0.17), m.p. 114-16°C, were separated ($\alpha \approx 1.70$).

The enantiomeric purity was checked by ^1H n.m.r. in deuteriochloroform in the presence of R(-)-2,2,2-trifluoro-1-(9-anthryl)ethanol (Pirkle's alcohol) in a 4 molar excess with respect to the enantiomer. The ^1H chemical shifts for each enantiomer are gathered in Table 5.

Table 5. ^1H chemical shifts of the enantiomers in the presence of Pirkle's alcohol.

Compound	H4	H5	H6	H7	CH(1)	CH ₃
Enantiomer(+)	7.63	7.21	6.94	5.91	8.23	2.00
Enantiomer(-)	7.61	7.21	6.94	5.91	8.18	1.94
$\Delta\delta = \delta\text{H}(+) - \delta\text{H}(-)$	0.02	0	0	0	0.05	0.06

The purity of enantiomers was also checked by circular dichroism. The rotatory power was measured in 95% ethanol at the concentration of $2.10 \cdot 10^{-3}$ g.ml⁻¹ using the 241 Perkin Elmer polarimeter (temperature, 25°C).

Racemization.— 1 ml of a solution of enriched (-)TMBM (4 mg) in 1,2-dimethoxyethane (1 ml) was introduced in a thermostated polarimeter cell at 70°C with an initial α value of -1.095. The rotatory power was measured each 15 min and after 540 min an α of -0.795 was obtained. The data were processed using the RACEM program.³⁰

X-Ray Crystallography.— The parameters describing the crystallographic analysis are given in Table 6, for crystals 1 $\equiv C^+$ and 2 $\equiv C^{+/-}$. Final atomic coordinates are given in Tables 7 and 8, according to the numbering scheme already presented. Figs. 11 and 12 were drawn with the program "Holes 1989" (Martínez-Ripoll, M.; Foces-Foces, C.; Hernández Cano, F. unpublished results). Atomic coordinates for the hydrogen atoms and anisotropic thermal parameters for non-hydrogen atoms, are available from the Director of the Cambridge Crystallographic Data Centre, University Chemical Laboratory, Lensfield Road, Cambridge CB2 1EW. Any request should be accompanied by

the full literature citation.

TABLE 6. Crystal analysis parameters at room temperature

Crystal data	1	2
Formula	2 (C ₂₅ H ₂₂ N ₆) · 7 H ₂ O	C ₂₅ H ₂₂ N ₆ · 3H ₂ O
Crystal habit	Transparent plate	Transparent, plate
Crystal size (mm)	0.27 × 0.20 × 0.13	0.33 × 0.23 × 0.20
Symmetry	Monoclinic, P2 ₁	Monoclinic, P2 ₁ /c
Unit cell determination:	Least-squares fit from 72 reflections ($\theta < 45^\circ$)	Least-squares fit from 88 reflections ($\theta < 45^\circ$)
Unit cell dimensions	18.6252(30), 13.3981(15), 9.9500(8) Å 90, 90.853(9), 90°	10.0364(5), 13.3774(7), 18.0879(11) Å 90, 92.904(6), 90°
Packing: $V(\text{Å}^3)$, Z $D_c(\text{g.cm}^{-3})$, M , $F(000)$ $\mu(\text{cm}^{-1})$	2482.7(5), 2 1.256, 939.08, 996 6.68	2425.4(2), 4 1.261, 460.54, 976 6.59
Experimental data		
Technique	Four circle diffractometer Bisecting geometry Graphite oriented monochromator: CuK α $\omega/2\theta$ scans, scan width: 1.6° Detector apertures 1.0x1.0°	
Total measurements	Up to 65° in θ	
Speed	1 min./reflec.	
Number of reflections:		
Independent	4451	4142
Observed	3375 [3 σ (I) criterion]	2367 (3 σ (I))
Standard reflections:	2 reflections every 90 minutes. Overall decay: 8%	2 reflexiones every 90 minutes No variation
Solution and refinement		
Solution	Direct methods	Direct Methods
Refinement	L.S. on F_{obs} , 5 blocks	L.S. on F_{obs} with 1 block
Parameters:		
Number of variables	829 (24 hydrogen parameters fixed)	403
Degrees of freedom	2546	1964
Ratio of freedom	4.1	5.9
H atoms	Difference synthesis	Difference synthesis (not located those 02 and 03 atoms)
Final shift/error	0.48	0.07
Weighting scheme	Empirical as to give no trends in $\langle w\Delta^2 \rangle$ vs. $\langle F_{\text{obs}} \rangle$ or $\langle \sin \theta / \lambda \rangle$	
Max. thermal value	$U_{11}[05]=0.191(9)\text{Å}^2$	$U_{33}(03)=0.188(5)\text{Å}^2$
Final ΔF peaks	0.38 e.Å^{-3}	0.35 e.Å^{-3}
Final R and R_w	0.067, 0.078	0.053, 0.061
Computer and programs	Vax11/750, XRAY76 ³¹ , MULTAN80 ³²	
Scattering factors	Int. Tables for X-Ray Crystallography ⁹	

ACKNOWLEDGMENTS

First of all, we want to recognize the invaluable help of Professor Jan Sandström in DNMR calculations. This work was supported by the 'Comisión Asesora de Investigación en Ciencia y Tecnología' of Spain (CAICYT, Projects no. 326/84 and PB-0281). One of us (C.L.) is indebted to the 'Secretaría General Técnica de la Consejería de Educación y Juventud de la Comunidad de Madrid' for a grant. Another of the authors (D.S.) thanks the Ministries of Education of Spain (MEC) and France (MRES) for a fellowship during her stage at the University of Marseilles. The ¹³C CP/MAS spectrum at 100.6 MHz of TMBM was recorded in Bruker Spectrospin AG, thanks to the courtesy of Dr. A. Torossian.

TABLE 7. FINAL ATOMIC COORDINATES: 1

Atom	x/a	y/b	z/c	Atom	x/a	y/b	z/c
C1	0.7401(3)	0.1000	0.3184(6)	C1'	0.5532(3)	0.6190(5)	0.3651(6)
M1	0.0803(3)	0.1791(4)	0.2553(5)	M1'	0.5904(3)	0.5388(4)	0.2982(5)
C2	0.0514(3)	0.2738(5)	0.2323(6)	C2'	0.5562(4)	0.4478(4)	0.2714(7)
N3	0.0984(3)	0.3302(4)	0.1712(6)	N3'	0.5985(3)	0.3866(4)	0.2057(5)
C3A	0.1596(4)	0.2731(5)	0.1522(6)	C3'A	0.6621(4)	0.4371(4)	0.1867(6)
C4	0.2233(4)	0.2988(6)	0.0918(7)	C4'	0.7235(4)	0.4032(6)	0.1230(7)
C5	0.2753(4)	0.2271(7)	0.0852(8)	C5'	0.7826(4)	0.4662(6)	0.1206(7)
C6	0.2669(4)	0.1342(6)	0.1392(7)	C6'	0.7787(4)	0.5598(6)	0.1818(8)
C7	0.2041(3)	0.1054(5)	0.2009(7)	C7'	0.7184(4)	0.5949(5)	0.2446(6)
C7A	0.1495(3)	0.1765(5)	0.2047(6)	C7'A	0.6589(3)	0.5308(4)	0.2464(6)
C8	-0.0199(4)	0.3039(6)	0.2757(9)	C8'	0.4941(4)	0.4258(6)	0.3211(8)
M11	0.0333(3)	0.1166(4)	0.4613(5)	M11'	0.5418(3)	0.5968(4)	0.5049(5)
C12	-0.0223(4)	0.0773(5)	0.5363(7)	C12'	0.4854(4)	0.6363(5)	0.5756(7)
M13	-0.0215(3)	0.1103(5)	0.6593(6)	M13'	0.4839(3)	0.6026(5)	0.6981(6)
C13A	0.0356(4)	0.1750(5)	0.6693(6)	C13'A	0.5401(3)	0.5351(5)	0.7108(6)
C14	0.0581(4)	0.2355(6)	0.7792(6)	C14'	0.5590(4)	0.4755(6)	0.6199(7)
C15	0.1181(4)	0.2915(5)	0.7647(8)	C15'	0.6161(4)	0.4122(6)	0.8041(7)
C16	0.1534(4)	0.2934(5)	0.6441(8)	C16'	0.6540(4)	0.4091(6)	0.6869(9)
C17	0.1327(4)	0.2379(5)	0.5328(6)	C17'	0.6379(4)	0.4680(5)	0.5759(7)
C17A	0.0713(3)	0.1798(4)	0.5485(6)	C17'A	0.5781(3)	0.5302(5)	0.5924(6)
C18	-0.0763(4)	0.0061(7)	0.4793(10)	C18'	0.4320(4)	0.7056(7)	0.5144(8)
N21	0.0685(3)	0.0028(4)	0.2906(5)	N21'	0.5907(3)	0.7133(4)	0.3447(5)
C22	0.0609(4)	-0.0451(5)	0.1666(7)	C22'	0.6353(3)	0.7702(5)	0.4265(6)
N23	0.0923(3)	-0.1316(4)	0.1624(6)	N23'	0.6551(3)	0.8514(5)	0.3660(6)
C23A	0.1240(3)	-0.1435(5)	0.2876(7)	C23'A	0.6242(3)	0.8485(5)	0.2390(7)
C24	0.1631(4)	-0.2260(5)	0.3388(9)	C24'	0.6296(4)	0.9181(5)	0.1345(8)
C25	0.1891(4)	-0.2197(5)	0.4650(8)	C25'	0.5934(4)	0.8956(6)	0.0189(9)
C26	0.1778(4)	-0.1370(6)	0.5448(7)	C26'	0.5509(4)	0.8090(6)	0.0045(8)
C27	0.1385(4)	-0.0558(5)	0.5005(7)	C27'	0.5457(4)	0.7411(5)	0.1072(7)
C27A	0.1101(3)	-0.0811(4)	0.3701(6)	C27'A	0.5843(3)	0.7628(5)	0.2225(6)
C28	0.0188(5)	-0.0006(6)	0.0553(8)	C28'	0.6593(4)	0.7437(6)	0.5660(7)
O1	0.1750(3)	0.5420(4)	0.1593(5)	O5	0.2713(4)	0.5480(9)	0.2775(8)
O2	0.3811(3)	0.6840(5)	-0.1104(6)	O6	0.2687(5)	0.5268(7)	0.5513(8)
O3	0.3937(4)	0.6278(6)	0.1733(8)	O7	0.2445(6)	0.6414(8)	-0.7151(11)
O4	0.1229(6)	0.6970(7)	-0.0306(8)				

TABLE 8. FINAL ATOMIC COORDINATES: 2

Atom	x/a	y/b	z/c	Atom	x/a	y/b	z/c
C1	0.6815(3)	0.5070(2)	0.2075(2)	C16	0.4439(5)	0.2664(3)	0.0699(2)
M1	0.5411(3)	0.5211(2)	0.2173(1)	C17	0.4954(4)	0.3500(3)	0.1077(2)
C2	0.4770(4)	0.4804(2)	0.2770(2)	C17 A	0.6250(3)	0.3446(2)	0.1348(2)
N3	0.3543(3)	0.5098(2)	0.2783(2)	C18	0.9464(5)	0.4072(4)	0.2283(3)
C3 A	0.3313(4)	0.5738(2)	0.2185(2)	N21	0.7368(3)	0.5875(2)	0.1645(1)
C4	0.2187(4)	0.6268(3)	0.1975(2)	C22	0.7638(6)	0.6816(2)	0.1941(2)
C5	0.2210(4)	0.6855(3)	0.1348(2)	M23	0.8249(3)	0.7389(2)	0.1487(2)
C6	0.3354(4)	0.6894(3)	0.0946(2)	C23 A	0.8410(3)	0.6821(2)	0.0852(2)
C7	0.4492(4)	0.6183(2)	0.1146(2)	C24	0.9003(4)	0.7094(3)	0.0206(2)
C7 A	0.4472(3)	0.5815(2)	0.1786(2)	C25	0.9003(4)	0.6402(3)	-0.0358(2)
C8	0.5452(6)	0.4119(4)	0.3309(3)	C26	0.8435(5)	0.5463(3)	-0.0281(2)
M11	0.7101(3)	0.4094(2)	0.1761(1)	C27	0.7844(4)	0.5176(2)	0.0361(2)
C12	0.8314(4)	0.3626(2)	0.1863(2)	C27 A	0.7852(3)	0.5871(2)	0.0930(2)
M13	0.8328(3)	0.2742(2)	0.1547(2)	C28	0.7231(6)	0.7115(3)	0.2690(3)
C13 A	0.7052(4)	0.2609(2)	0.1230(2)	O1	0.1752(4)	0.4494(2)	0.3841(2)
C14	0.6529(5)	0.1780(2)	0.0848(2)	O2	0.0146(4)	0.6018(2)	0.3623(2)
C15	0.5230(5)	0.1819(3)	0.0595(2)	O3	0.2231(6)	0.4704(5)	0.5481(3)

REFERENCES

- Mislow, K.; Gust, D.; Finocchiaro, P.; Boettcher, R.J. Topics in Current Chemistry, 1974, 47, 1.
- Gust, D.; Mislow, K. J. Am. Chem. Soc., 1973, 95, 1535.
- Mislow, K. Acc. Chem. Res., 1976, 9, 26.
- Dunitz, J.D. X-Ray Analysis and the Structure of Organic Molecules, Chap. 10, Cornell University Press, Ithaca, 1979.
- Kurland, R.J.; Schuster, I.I.; Colter, A.K. J. Am. Chem. Soc., 1965, 87, 2279.
- Bye, E.; Schweizer, W.B.; Dunitz, J.D. J. Am. Chem. Soc., 1982, 104, 5893.
- Murray-Rust, P.; Burgi, H.B.; Dunitz, J.D. J. Am. Chem. Soc., 1975, 97, 921.
- Burgi, H.B.; Dunitz, J.D. Acc. Chem. Res., 1983, 16, 153.

9. International Tables for X-Ray Crystallography, Vol. IV, Birmingham: Kynoch Press, England (Present distributor D. Reidel, Dordrech) (1974).
10. Juliá, S.; Sala, P.; del Mazo, J.M.; Sancho, M.; Ochoa, C.; Elguero, J.; Fayet, J.P.; Vertut, M.V. J. Heterocycl. Chem., 1982, 19, 1141.
11. Claramunt, R.M.; Hernández, H.; Elguero, J.; Juliá, S. Bull. Soc. Chim. Fr., 1983, II, 5.
12. Claramunt, R.M.; Elguero, J.; Meco, T. J. Heterocycl. Chem., 1983, 20, 1245.
13. Avila, L.; Juliá, S.; del Mazo, J.M.; Elguero, J. Heterocycles, 1983, 20, 1787.
14. Juliá, S.; del Mazo, J.M.; Avila, L.; Elguero, J.; Org. Prep. Proc. Int., 1984, 16, 299.
15. Juliá, S.; Martínez-Martorell, C.; Elguero, J. Heterocycles, 1986, 24, 2233.
16. Elguero, J.; Claramunt, R.M.; Garcerán, R.; Juliá, S.; Avila, L.; del Mazo, J.M. Magn. Reson. Chem., 1987, 25, 260.
17. Ballesteros, P.; Claramunt, R.M.; Elguero, J.; Roussel, C.; Chemlal, A. Heterocycles, 1988, 27, 351.
18. Claramunt, R.M.; Elguero, J.; Fabre, M.J.; Foces-Foces, C.; Cano, F.H.; Fuentes, I.H.; Jaime, C.; López, C. Tetrahedron, in press.
19. Jaime, C.; Virgili, A.; Sanz, D.; Faure, R.; Claramunt, R.M.; López, C.; Elguero, J. unpublished results.
20. Alkorta, I.; Elguero, J.; Goya, P.; Roussel, C. Chromatographia, 1989, 27, 77 and references therein.
21. Allen, F.H.; Kennard, O.; Taylor, R. Acc. Chem. Res., 1983, 16, 146 and references therein (Version April 1989).
22. Lockhart, J.C.; McDonnell, M.B.; Clegg, W.; Stuart-Hill, M.N. J. Chem. Soc., Perkin Trans. 2, 1987, 639 and 1621; Brock, C.P.; Das, M.K.; Minton, R.P.; Niedenzu, K. J. Am. Chem. Soc., 1988, 110, 817.
23. Declercq, J.P.; Van Meerssche, M. Acta Crystallogr., 1984, C40, 1098.
24. Cameron, T.S.; Dahlen, B. J. Chem. Soc., Perkin Trans. 2, 1975, 1737.
25. Cameron, T.S.; Howlett, K.D.; Miller, K. Acta Crystallogr., 1978, B34, 1639.
26. Allen, D.W.; March, L.A.; Nowell, I.W. J. Chem. Soc., Dalton Trans., 1984, 483.
27. Lindner, K.; Saenger, W. Acta Crystallogr., 1982, B38, 203.
28. Croasmun, W.R.; Carlson, R.M.K. Two-Dimensional NMR Spectroscopy, VCH Publishers, New York, 1987.
29. Chiral Liquid Chromatography, Lough, W.J. Ed., Blackie, London, 1989.
30. Roussel, C.; Adjani, M.; Chemlal, A.; Djafri, A. J. Org. Chem., 1988, 53, 5076.
31. Stewart, J.M.; Machin, P.A.; Dickinson, C.W.; Ammon, H.L.; Heck, H.; Flak, H. 'The X-Ray System', Technical Report TR-446, Computer Science Center, Maryland (1976).
32. Main, P.; Fiske, S.J.; Hull, S.E.; Lessinger, L.; Germain, G.; Leclerc, J.P.; Woolfson, M.M. 'Multan 80 System', University of York, England (1980).